



Numerical Investigation in Nitinol Lattice Stability and Safe Usage in Replacing Hard Tissue

Soha S. Hiadrah¹, Zina A. Al shadidi^{2*}

¹Department of Physics, Faculty of Education, University of Abian, Yemen

²Department of Physics, Faculty of Education, University of Aden, Yemen

Received: 24/2/2022

Accepted: 21/8/2022

Published: 30/6/2023

Abstract:

NiTi (also called Nitinol) transforms from cubic (austenite) to monoclinic (martensite), and vice versa, owing to the shape memory effect and superelasticity. Nitinol has a large number of biomedical applications because of its low elastic modulus close to that of natural bone material and good resistance to corrosion and fatigue, in addition to the transformation temperatures of nitinol that are close to body temperature. It has many other important applications, such as in the aircraft industry. In all these important applications, especially medical applications, Nitinol stability is an important factor for safety. Our goal is to study the stability of NiTi by calculating the phonon dispersion relation to obtain an accurate understanding of the mechanically unstable phases of the NiTi alloy. The dispersion relation for the cubic and monoclinic phases was studied and coded using MATLAB to make a clear consideration of the dispersion relation and its optical and acoustic branches. Moreover, the density of the state and energy from the lattice vibrations were calculated.

The crystal is found to be stable by the anharmonic part of the interactions. The austenite phase is stable up to (300 K). While it is not above (300 K). Any extra energy due to temperature changes caused the transformation to the martensite phase. The positive phonon modes indicate that the monoclinic phase is stable against energy perturbations. When the thermal vibration energy was calculated $F_{\text{vib}}(T) = 54.8 \text{ meV}$ for the cubic phase and $F_{\text{vib}}(T) = 38 \text{ meV}$ in the case of the monoclinic phase at $T = 300 \text{ K}$. In both cases, it was less than 5 eV. There are no broken bonds owing to the energy of vibration.

Keywords: Nitinol, lattice stability, density of states, phonons, MATLAB.

1-Introduction:

Shape memory alloys are smart materials consisting of two or more different metals. They exhibit two unique properties: pseudoelasticity and shape memory effects, such that they undergo a structural phase transformation when heated or subjected to appropriate stress [1]. The transformation from the austenite lattice to the martensite lattice can be described as a deformation (because there is no diffusion). Nitinol has excellent potential for use as a biomaterial, compared to other conventional materials because of its shape memory and superelastic properties. The main medical applications of NiTi alloys are in dental, orthopedic, vascular, neurological, and surgical fields [2], [3]. Therefore, Nitinol stability is regarded as an articulation point at which we must stand to ensure patient safety.

*Email: zabaqer@yahoo.com

Phonons are essential in explaining how and when shape memory and pseudelasticity process. Moreover, the NiTi alloy is a conventional system for studying soft modes, one observes huge unit cell changes across the phase transformation. Such unit cell variations could bring the crystal to another energy minimum and change the phonon behavior.

Yangthaisong [4] computed the structural and electronic properties of BaHfO₃ within the local density approximation. The phonon dispersion curves of BaHfO₃ were also calculated. Cousland et al.[5] studied the mechanical properties of zirconia, cubic YSZ, and YSZ doped with Ti, Mn, Ca, and Ni oxides using density functional theory (DFT) calculations. Yang and Shang [6] studied the Ab Initio Study of Martensitic Transformation in NiTiPt high-temperature shape memory alloys.

Herget et al. [7] studied the generalized phonon density of states of the structural phases of nearly equiatomic $Ni_{50.5}Ti_{49.5}$, by means of inelastic neutron scattering for the first time, and macroscopic properties such as the specific heat and the mean-square amplitudes of lattice vibrations. They found only two pronounced peaks and no gaps between the acoustic and optical modes. The specific heat calculated from the martensitic PDOS agrees with the experimental results at low temperatures, where the calculations hold only within the limits of the harmonic approximation.

Kadkhodaei and van de Walle[8] calculated the thermal properties of the mechanically unstable phases of PtTi and NiTi shape memory alloys using the first-principles. The thermodynamic properties of the B2 phase of NiTi, B2, and B19 phases of PtTi were calculated using the P4 method because of the existence of harmonic phonon instabilities, whereas the thermodynamic properties of the B19 phase of NiTi were calculated using the standard first-principles harmonic approximation. Huang et al. [9] computed the phonon dispersion relation of NiTi in a simple cubic B2 structure using first-principles density-functional perturbation theory with pseudopotentials and a plane-wave basis set. Lattice instabilities occur throughout the entire Brillouin zone.

In this study, all phases and, accordingly, all the variables are seen from one point of view and belong to one theory, which is the density function theory (DFT).

Our code of calculations was based upon our model, which depends on the principal calculations of lattice dynamics on a harmonic oscillator (atoms). Atoms moved according to the relative displacements in the unstable eigenvector related to the lattice symmetry, to calculate the force matrices and the atomic displacement associated with the eigenvector of the dynamical matrix in the K-space. As the cubic NiTi lattice changes its phase to monoclinic, using the energy gained from thermal changes or the exerted stress, it is very important to examine the NiTi stability. This research highlights the amount of energy released from atomic vibrations caused by heat changes or stresses.

Lattice vibrations increase as the force acting on the lattice increases. This leads to the generation of waves, known as elastic waves, inside the crystal. These waves, in turn, excite all the atoms in the crystal lattice in a collective movement known as the normal pattern of lattice vibrations. The pattern of vibration in three dimensions for a finite lattice is described by the following equation:

$$m\ddot{u} + Ku = 0 \quad \text{--- (1)}$$

Where: m , u , and K are matrices of the masses, displacements, and spring constants, respectively. The NiTi alloy had a B2 cubic structure. Therefore, it is suitable to write the force equations in three dimensions as a series of combinations of the (110) and (011) planes.

In the (110) plane, the spring constants depend on the angle between the x-axis and the line between the atom at the origin and any atom. Therefore $K_{i,j,k,1}$, $K_{i,j,k,2}$, $K_{i,j,k,3}$, and $K_{i,j,k,4}$ are the spring constants in the 0 deg, 45 deg, 90 deg, and 135 deg. Each mass was also connected to the base of the material vertically with springs $K'_{x,y}$, $K'_{y,x}$, $K'_{y,z}$, $K'_{z,y}$. The subscripts x, y, and z denote the spring stiffness in the x, y, and z directions, respectively [10].

The small-amplitude displacements in three dimensions (x, y, and z) are (p+i, q+j, r+k), respectively are:

$$\begin{aligned}
 m_{i,j} \ddot{u}_{p+i,q+j} = & k_{i,j,1}(u_{p+i+1,q+j} - u_{p+i,q+j}) \\
 & + 0.5k_{i,j,2}(u_{p+i+1,q+j+1} - u_{p+i,q+j} + u_{p+i+1,q+j+1} - u_{p+i,q+j}) \\
 & + 0.5k_{i,j,4}(u_{p+i-1,q+j+1} - u_{p+i,q+j} - u_{p+i-1,q+j+1} + u_{p+i,q+j}) \\
 & + k_{i-1,j,1}(u_{p+i-1,q+j} - u_{p+i,q+j}) \\
 & + 0.5k_{i-1,j-1,2}(u_{p+i-1,q+j-1} - u_{p+i,q+j} + u_{p+i-1,q+j-1} - u_{p+i,q+j}) \\
 & + 0.5k_{i+1,j-1,4}(u_{p+i+1,q+j-1} - u_{p+i,q+j} - u_{p+i+1,q+j-1} + u_{p+i,q+j}) \\
 & + k'_{x,i,j}(0 - u_{p+i,q+j}) \quad \text{-----} \quad (2)
 \end{aligned}$$

Similarly, the force exerted in the (011) and (101) planes are calculated to each solution of the three equations, which are assumed to be sinusoidal wave equations of the form:

$$u_{p+i}(t) = A_{i,j} e^{i((p+i)\gamma_x + (q+j)\gamma_y - \omega t)} \quad \dots \dots \dots (3a)$$

$$u_{p+i}(t) = B_{i,j} e^{i((p+i)\gamma_x + (q+j)\gamma_y - \omega t)} \quad \dots \dots \dots (3b)$$

$$u_{q+i}(t) = C_{j,k} e^{i((q+j)\gamma_y + (r+k)\gamma_z - \omega t)} \quad \dots \dots \dots (3c)$$

Where: $A_{i,j}$, $B_{i,j}$, and $C_{j,k}$ are the wave amplitudes, ω is the wave frequency, and $\gamma_x, \gamma_y, \gamma_z$ are the x, y, and z components of the wavevector, respectively

$K_{i,j,k,1}$, $K_{i,j,k,2}$, $K_{i,j,k,3}$, and $K_{i,j,k,4}$ are calculated according to the first and second neighbors. The first neighbors are of different types of atoms; therefore, according to the NiTi structure $K_{i,j,k,1}$ and $K_{i,j,k,3}$ equals $(\frac{m_1}{m_2}) = 1.226$, related to the eight nearest neighbors; where $K_{i,j,k,2}$, and $K_{i,j,k,4}$ are equal to $(\frac{m_1}{m_1})=1$, and are related to the 12 nearest neighbors.

1-1 vibration energy and density of states

Gibbs free energy changes initiate a chemical reaction, indicating whether the reaction is spontaneous, and how much energy is needed for the reaction.

Gibbs free energy is defined as [11]:

$$G(P, V, T) = U - TS + PV \quad \dots \dots \dots (4)$$

Where: U is the internal energy, S is the entropy, P represents the pressure, and V is the crystal volume. The internal energy may be expressed as $U = U_0 + U_{vib}$, where U_0 is the static internal energy and U_{vib} is the vibration internal energy. The PV in Equation (4) was neglected because of the small change in volume. Helmholtz free energy is given by the following equation:

$$F(T) = U - TS = U_0 + F_{vib}(T) \dots \dots \dots (5).$$

The vibration energy is written as follows [8], [9]:

$$F_{vib}(T) = 3NK_B T \int_0^\infty d(\omega)g(\omega) \ln \left[2 \sinh \left(\frac{\hbar\omega}{2K_B T} \right) \right] \quad \dots \dots \dots (6)$$

Where: K_B is Boltzmann's constant, and $d(\omega)g(\omega)$ represents the density of states per unit frequency ω , $\omega + d\omega$ is $d(\omega)g(\omega)$.

$$g(\omega) = \frac{1}{2\pi} \frac{1}{(d\omega/dq)}$$

The heat capacity is given by [11], [12]:

$$C_v(T) = \frac{11}{4K_B T^2} \int_0^\infty d(\omega) g(\omega) \frac{\hbar\omega^2}{\sinh^2\left(\frac{\hbar\omega}{2K_B T}\right)} \dots \dots \dots (7)$$

2- Methodology:

The NiTi primitive cell has one atom in the cubic austenite phase. There are two types of dispersion branches (acoustic and optical) for each polarization mode in one direction. The acoustic branch has two transverse modes (TA) and one longitudinal mode (LA). The same division occurred with the optical branch, which has two transverse modes (TO) and one longitudinal mode (LO). For n atoms per primitive cell, d degrees of freedom (nxd) branches found for each k value. The number of acoustic branches equals (d), and the remaining is optical. For the diatomic system (NiTi), with d=3 (in three dimensions), there are six branches, two longitudinal and four transverse. In the present calculations, the chosen symmetry direction was [110].

3- Results

3-1 Phonon dispersion relation

Calculations of the phonon density of states show the existence of vibrational modes at the frequencies mentioned at the boundary of the Brillion zone. The discreteness of phonons for the B2 cubic lattice is shown in Figure (1) by high symmetry points, which refer to the high-frequency section of the optical and acoustic branches. In reality, phonons are densely packed, leading to a quasi-continuous distribution [13].

The calculated density of state is regarded as a cubic and monoclinic lattice using the linear spring model. At the transition temperature of 300K, where the restoring force constant for the first neighbor is assumed to be equal:

$$\frac{c_1}{c_2} = \frac{m_1}{m_2} = 1.226$$

Where: m_1 is Ni atomic mass =58.693amu, m_2 is the atomic mass of Ti =47.867amu, and $a_0 = 3.015 \text{ \AA}^0$

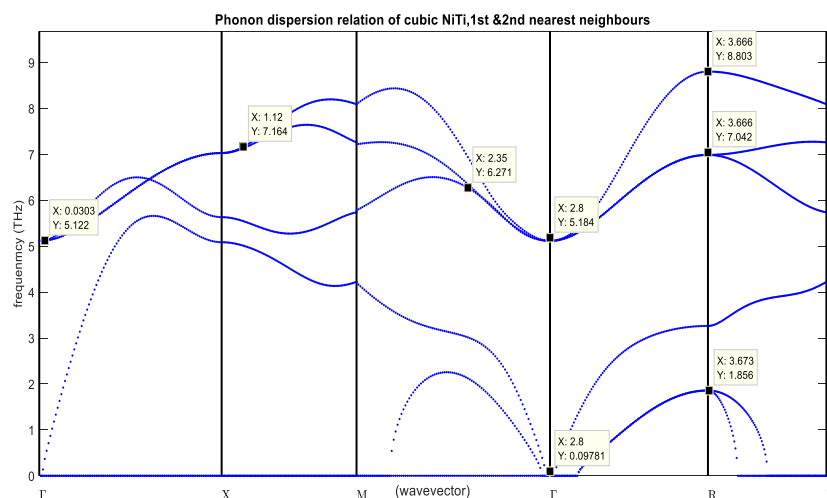


Figure 1: phonon dispersion of cubic NiTi, only real part of frequency.

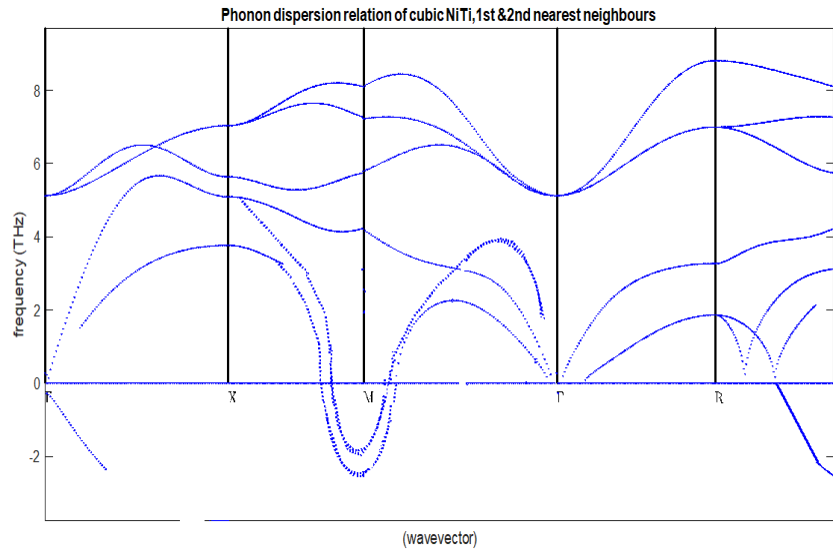


Figure 2: The dispersion relation of cubic in NiTi, real and imaginary parts of frequency

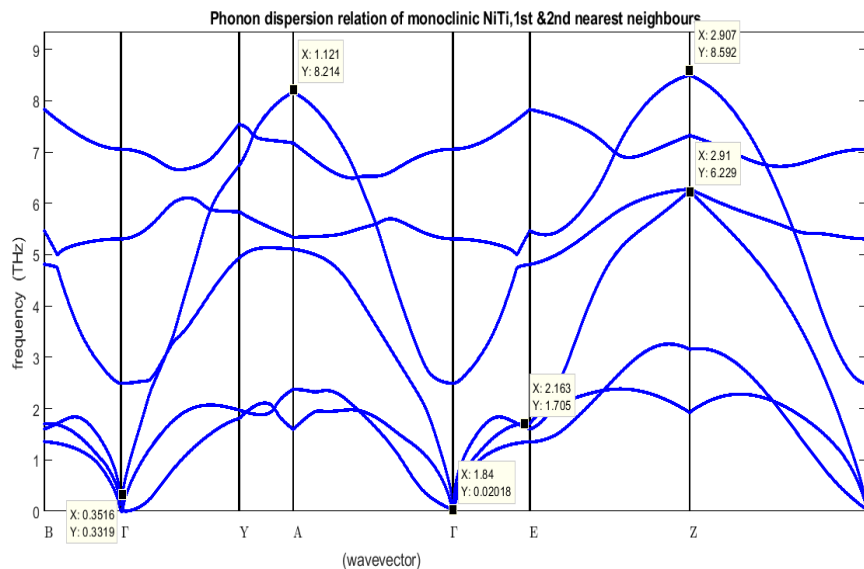


Figure 3: The dispersion relation of monoclinic in NiTi

The phonon dispersion was plotted along the high-symmetry directions in the first Brillouin zone. Figure 1 shows the dispersion relation for the high-temperature austenite cubic structure (only the real part of the frequency). Figure 2, shows the dispersion relation with both real and imaginary components of the frequency to clarify the soft modes through a comparison between Figures 1 and 2. The high-symmetry lines in Figure 1 and 2, start at Γ (0,0,0) point, going through the Γ , X, M, Γ , R, and M points. While in Figure 3, plotted for the low-temperature Martensite monoclinic structure, the high symmetry points were B, Γ , Y, A, Γ , E, Z, Γ .

NiTi is regarded as a very active material owing to its transformation from cubic to monoclinic. According to Equation (3), the NiTi cubic structure transforms into a monoclinic structure through approximately rigid shifts of alternate (110) planes along the $(1\bar{1}0)$ direction, owing to the temperature change. The stability of NiTi was examined by calculating the

phonon modes across the Brillion zone to determine the nature of the local structural fluctuations in both phases (in the cubic and monoclinic phases).

In Figure 1, the splitting and merging energy states are shown. Two of the splitting points were at Γ high symmetry points (5.184 and 0.0978)THz and the other at (5.122,7.164, 7.042, and 1.856)THz. One merging point is observed at a frequency equal to (6.217)THz. The maximum frequency point was at (8.803)THz. According to Parlinski [14], the imaginary frequency for the unstable mode is represented as a negative value or what is called (the soft modes), as shown in Figure 2. The origin of phonon softening is attributed to the electron phonon coupling of nested electron states on fermi surfaces [13]. According to this curve, the B2 cubic lattice tends to transform into another phase when energy is received from an external source. Figure 3 shows that there is nothing beyond zero frequency; in other words, all the acoustic and optical branches are positive, which is conclusive evidence of phase stability.

Figure 3 shows that there are no modes beyond zero frequency; in other words, all the acoustic and optical branches are positive, which is conclusive evidence of phase stability against any phonon-like perturbation. On the other hand, the split states at Γ symmetry points at frequencies (46.98 and 44.98)GHz, and on Z high symmetry point at (6.24)THz , also at (1.705)THz near the E high symmetry point . Many temporary merging and splitting points are shown in Figure 3; however, there are positive frequency fluctuation points. The highest frequency point in the monoclinic dispersion relation appears at (Z, and A) high symmetry points at (8.214, and 8.592)THz, respectively.

3-2 density of states

The thermodynamic properties of the high-temperature B2 cubic structure and (B19/) monoclinic structure were studied using a linear spring model. For NiTi, the electronic states below the Fermi level are mostly contributed by the Ni-d states, while electronic states above the Fermi level originate mainly from Ti-d states [12].

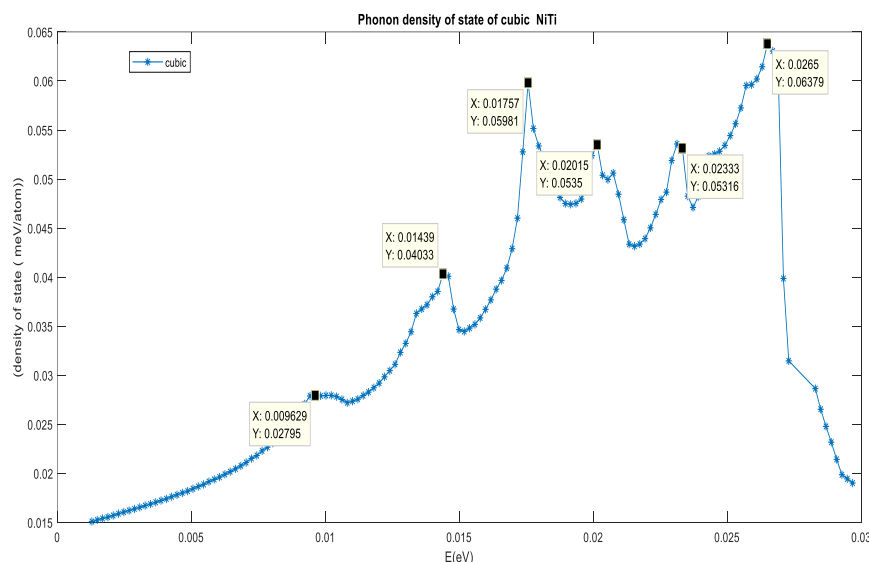


Figure 4 : phonon dispersion relation of NiTi, cubic Austenite B2 cubic structure with 1st and 2nd nearest neighbors, $C = \frac{c_1}{c_2} = \frac{m_1}{m_2} = 1.226$

In Figure 4, the density of states for the 1st and 2nd nearest neighbors in the NiTi cubic structure were calculated by calculating the frequencies $\omega = \sqrt{\frac{C}{m}}$.

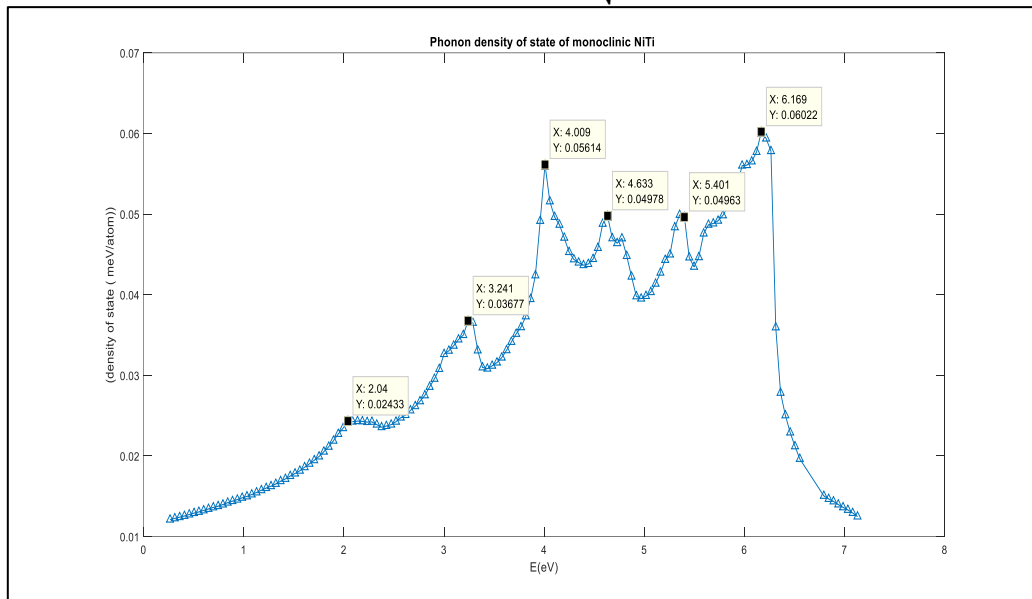


Figure 5: density of state for Martensite B19' monoclinic structure with $\frac{C_1}{C_2} = \frac{m_2}{m_1} = 1.226$

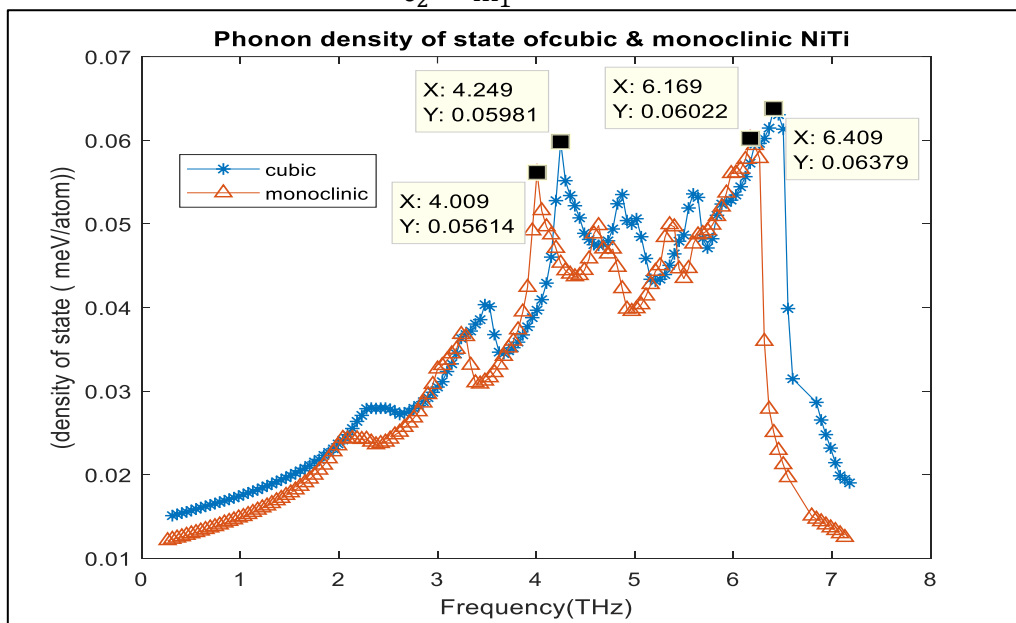


Figure 6: density of state for Austenite Cubic & Martensite B19' monoclinic structure

Comparing the cubic and monoclinic density of state, and from the figures above, it is clear that the cubic phase has a higher density of state peaks (0.05981 meV/atom) at frequencies equal to (4.249 THz) and (0.06379 meV/atom) at a frequency equal to (6.409 THz). It is equal to (0.05614 meV/atom) at frequencies of (4.009 THz) and (0.060229 meV/atom) at a frequency of 6.169 THz. These results indicate that the higher-symmetry cubic phase has a larger vibration energy for each atom.

Our results agree with the results of Hung, Rabe, and Ackland [9].

3-2 chemical stability:

The thermal vibration energy at (300 K) was calculated using Equation (6). It was $F_{\text{vib}}(T) = 54.8$ meV for the cubic phase, and $F_{\text{vib}}(T) = 38$ meV for the monoclinic phase, which is less than the lowest binding energy required to break the NiTi bond [15], [16].

This indicates that the transformation of NiTi is stable. In addition, there are no broken bonds owing to the energy of vibration. Our results are in agreement with those of Herget et. al. [7].

5- conclusions:

The structure and dynamical properties of the austenite and martensite phases were studied using ab initio calculations.

In Figure 1, the phonon dispersion relation of the high-symmetry B2 cubic lattice spread up to 8.803 THz at . There are degenerate acoustic and optical modes at $\Gamma(0,0,0)$ reciprocal lattice point and optical degenerate mode at $X(0, \frac{1}{2}, 0)$ reciprocal lattice point.

The crystal is stabilized by the anharmonic part of the interactions. When all the eigenvalues are positive, the local potential is a single minimum. Thus, the austenite phase is stable at (300 K). While it is not above (300 K), it has a negative frequency value in the dispersion relation curves. The negative values came from the imaginary parts of the wave accompanied by lattice vibrations because of electron-phonon coupling. This indicates that any extra energy due to temperature changes, caused the transformation to the martensite phase.

In Figure (3), ab initio calculations were performed for the martensite (B19') structure. The positive phonon modes indicate that the monoclinic phase is stable against energy perturbations.

When the thermal vibration energy was calculated $F_{\text{vib}}(T) = 54.8$ meV for the cubic phase and $F_{\text{vib}}(T) = 38$ meV in the case of the monoclinic phase at $T = 300$ K, which is less than the lowest binding energy required to break the NiTi bond [14,15]. In both cases, it was less than 5 eV, which is the numerical evidence for the automatic austenite-to-martensite transformation in NiTi at room temperature.

This indicates that the transformation of NiTi is stable. In addition, there are no broken bonds owing to the energy of vibration.

References

- [1] Matti Nasir Makdisi, Zina Al -Shadidi, "New Method For Evaluating Gibbs Free Energy In Shape Memory Alloys," *Iraqi Journal of Science*, vol. 51, no. 2, pp. 301-307, 2010 .
- [2] L. Petrini and F. Migliavacca, *Biomedical Applications of Shape memory Alloys*, Hindawi Publishing, 2011 .
- [3] Y. Zheng, *Introduction of antibacterial function into biomedical TiNi shape memory alloy by the addition of element Ag*, 2011 .
- [4] A. Yangthaisong, "Electronic and lattice vibrational properties of cubic BaHfO₃ from first principles calculations," *Physics Letters A*, vol. 377, p. 927–931, 2013 .
- [5] G.P. Cousland, X. Y. Cui, A.E.Smith, A.P..J. Stampfi, C.M.Stampfi, "Mechanical properties of zirconia, dopedand undoped Yttria_stabilized cubic Zirconia from first principles," *Journal of Physics and Chemistry of solids*, vol. 122, pp. 51-71, 2018 .
- [6] X. Yang , J. Shang, "Ab Initio Study of Martensitic Transformation in NiTiPt High Temperature Shape Memory Alloys," *Appl. Sci.*, vol. 11, no. 15, p. 6878, 2021 .
- [7] G. HERGET, M. MULLNER, J . B. SUCK, R. SCHMID, and H. WIPF., "Phonon Spectra of the Memory Alloy NiTi," *Europhysics Letters*, vol. 10, no. 1, pp. 49-54, 1989 .
- [8] S. Kadkhodaei, A.V. de Walle, "First-principles calculations of thermal properties of the mechanically unstable phases of the PtTi and NiTi shape memory alloys," *Acta Materialia*, vol. 147, pp. 296-303, 2018 .

- [9] X. Huang, C. Bungaro, V. Godlevsky, and K. M. Rabe, "Lattice instabilities of cubic NiTi from first principles," *Physical Review B*, vol. 65, pp. 63.20.2e, 64.60.2i, 2001 .
- [10] Z. J. Cao, *One and Two-Dimensional Mass Spring Computational Model for Phononic Band Gap Analysis*, Ontario, Canada: the University of Waterloo, 2009 .
- [11] T. Huan, *Evaluation of crystal free energy with lattice dynamics*, USA: Institute of Materials Science, University of Connecticut, Storrs, 2018 .
- [12] X. Luo, W. Zhou, S. V. Ushakov, A. Navrotsky, and A. A. Demkov, "Monoclinic to Tetragonal Transformations in Hafnia and Zirconia: A Combined Calorimetric and Density Functional Study," *Physical Review B*, vol. 80, pp. 64.60.i- 63.20.d, 2009 .
- [13] D. Holec, M. Friák, A. Vlček, and J. Neugebauer, "Ab initio study of point defects in NiTi-based alloys," *Physical Review B*, pp. 1-7, 2013 .
- [14] K. Parlinski, M. Parlinská and R. Gotthardt, "Phonons in austenite and martensite NiTi crystals," *J. Phys. IV France*, vol. 112, pp. 635-638, 2003 .
- [15] F. Caruso, D. R. Rohr, M Hellgren, X. Ren , P. Rinke, "Bond Breaking and Bond Formation: How electron Correlation is Captured in Many- Body Perturbation Theory and Density- Functional Theory," *physical review letters*, vol. 110, pp. 146403-1 - 146403-5, 2012 .
- [16] Hatcher. N ., Kontsevoi Yu. And Freeman A.J, "Martensitic Transformation Path of NiTi," *Physical Review B.*, vol. 79, pp. 020202-1 - 020202-4, 2009.